Internal Wetting in Three-Component Polymer Blends

Chuck Yeung,† Rashmi C. Desai,† and Jaan Noolandi*,‡

Department of Physics, University of Toronto, Toronto, Ontario M5S 1A7, Canada, and Xerox Research Centre of Canada, 2600 Speakman Drive, Mississauga, Ontario L5K 2L1, Canada

Received May 25, 1993; Revised Manuscript Received September 29, 1993®

ABSTRACT: We determine the interfacial properties of a three-component polymer blend in three-phase coexistence. We discuss how the presence of the third component affects the behavior of the interface between two phases and demonstrate the existence of a wetting transition in which one of the minority phases wets the other. Our results indicate that both first- and second-order wetting transitions can occur and that the range of parameters in which the wetting transition is second order may be experimentally accessible.

I. Introduction

The ability to characterize polymer interfaces is of both theoretical and technological importance. For example, if there is great deal of overlap between two types of polymers at an interface, the resulting entanglements can lead to a stronger material. More generally the interfacial properties of polymer blends can determine whether the material is useful for a particular purpose.[1] On the other hand, the thickness of a polymer interface relative to that of a simple liquid and the applicability of mean-field theory make polymer systems a good testing ground for theoretical ideas. One example is a three-component polymer blend. Helfand has recently discussed such a system in which two of the components are miscible while the third component is immiscible with the other two.[2] It was found that the presence of the additional component, even at small volume fractions, can reduce the interfacial tension. Another example is the interaction of a two-component polymer blend with a rigid wall. Schmidt and Binder[3] and Carmesin and Noolandi[4] found that such a system can undergo a first-order wetting transition.

Wetting phenomena are relevant to many processes of practical importance where typically a macroscopically thick layer of liquid covers the entire surface of a solid in a thermodynamically stable manner. Wetting requires the presence of three stable phases,[5] not necessarily in full thermodynamic equilibrium. For example, a solid substrate is generally not in equilibrium with an adsorbed two-phase fluid mixture since a low vapor pressure solid sublimates slowly. However, full thermodynamic equilibrium is achieved on an experimental time scale for three-phase simple fluid mixtures. The qualitative wetting behavior is the same in both cases.

In this paper we determine the interfacial behavior of a three-component polymer blend at three-phase coexistence. We illustrate this with an experiment performed by Hobbs et al.[6] where they studied a polymer blend, polystyrene (PS), Bisphenol A polycarbonate (PC), and poly(butylene terephthalate) (PBT), at three-phase coexistence, with PBT being the majority phase. It was found that the PC forms an encapsulating layer around small domains of PS. On the other hand, for other three-component polymer blends, it was found that the two minority components form separate domains.

To describe the more general case, we label the intervening phase as A (e.g., PC), the majority phase as B (e.g., PBT), and the encapsulated phase as C (e.g., PS). Hobbs et al. interpreted their data in terms of the spreading coefficient of the A phase on the interface between the B and C phases. They confirmed that this was the important parameter by using a random copolymer as the intervening phase so that the spreading coefficient could be adjusted in a controlled manner. If the spreading coefficients were positive, encapsulated domains were formed, while for negative spreading coefficients, separate small domains were formed.

The spreading coefficient of the A phase on the B–C interface is simply $S = \gamma_{BC} - \gamma_{AC} - \gamma_{AB}$ where γ_{pq} is the surface tension of an interface between the p and q phases. The properties of the polymer blend are therefore controlled by the surface tensions of the three interfaces. If $\gamma_{AB} + \gamma_{AC} > \gamma_{BC}$ ($S < 0$) partial wetting will occur, there will be some enrichment of the A phase at the B–C interface, but the thickness of the interface will be microscopic. If $\gamma_{AB} + \gamma_{AC} < \gamma_{BC}$ ($S > 0$), complete wetting will occur, and a macroscopic wetting layer of the A-rich phase will form between the B and C phases. In this case the domains of C will be encapsulated by an A-rich layer.

Therefore, there can be a transition from partial to complete wetting as the parameters are varied. The wetting transition is first order if there is a discontinuous jump in the thickness of the wetting layer, while it is second order if the thickness grows continuously from microscopic to macroscopic size. Which of these occurs depends on the interactions between the phases. First-order wetting transitions are more commonly observed experimentally.[7] For reviews of equilibrium wetting, see refs 8–10.

Therefore, to understand the interfacial properties of the three-component polymer blend, we need to obtain the surface tensions of the interface between the different phases in the presence of the third component. To do so, we use a numerical self-consistent-field method so that, rather than having a rigid wall, all three phases are in local equilibrium near the interface. We find that a wetting transition can occur in which one of the majority phases wets the other. We focus on two features. First, we determine how the presence of the third component affects the behavior of the interface between the two phases. We calculate the polymer concentration profiles and discuss the overlap of the different phases. We determine the surface tension and relate it to the surface tension of the pure two-component interface. We find that the presence of the third component reduces the surface tension of the three-component interface from its two-component value. Second, we discuss the nature of the wetting transition in the three-component blend. In particular, we show that first-order wetting transitions occur. Our results also

† University of Toronto.
‡ Xerox Research Centre of Canada.
® Abstract published in *Advance ACS Abstracts,* December 1, 1993.

0024-9297/94/2227-0055$04.50/0

indicate that a second-order wetting transition can occur, and we find that the range of parameters in which the wetting transition is second order is fairly large and may be experimentally accessible.

II. Model and Method

To model the three-component homopolymer system, we assume that both the interaction energy and the configurational entropy are of the Flory–Huggins form. The total interaction energy is $W = \rho_0 \int d\mathbf{r}\, f(\phi(\mathbf{r}))$ where the interaction energy per monomer f (in units of $k_B T$) is given by

$$f(\phi(\mathbf{r})) = \chi_{AB}\phi_A(\mathbf{r})\,\phi_B(\mathbf{r}) + \chi_{AC}\phi_A(\mathbf{r})\,\phi_C(\mathbf{r}) + \chi_{BC}\phi_B(\mathbf{r})\,\phi_C(\mathbf{r}) \quad (2.1)$$

and the χ's are the Flory interaction parameters, ϕ_p is the local volume fraction of polymer p, and ρ_0 is the density of the polymer in units of monomer segments per unit volume and is assumed to be the same for A, B, and C. The configurational entropy (in units of k_B) is

$$S = \rho_0 \int d\mathbf{r} \left[\frac{1}{Z_A}\phi_A(\mathbf{r}) \ln \phi_A(\mathbf{r}) + \frac{1}{Z_B}\phi_B(\mathbf{r}) \ln \phi_B(\mathbf{r}) + \frac{1}{Z_C}\phi_C(\mathbf{r}) \ln \phi_C(\mathbf{r})\right] \quad (2.2)$$

where Z_p is the polymerization of a chain of type p. The conformational entropy, however, is not approximated by a square gradient expansion but is obtained from the full conformational distribution function. The distinction between the more exact calculation and the square gradient approximation should not produce qualitative differences if χZ is not too large. This was demonstrated in ref 4 for the case of wetting in the presence of a wall. However, it will produce quantitative differences which can be important for comparison with experiments. Note that all terms in the interaction energy are short ranged. Complete details are given in the appendix.

The Flory interaction parameters χ_{pq} are chosen so that an A-rich phase, a B-rich phase, and a C-rich phase are at coexistence. This requires that $\chi_{pq}Z_q > 2$ for all p and q. Since we assume that A is the intervening phase between the B and C phases, we choose $\chi_{AB} < \chi_{BC}$ and $\chi_{AC} < \chi_{BC}$. The coexistence values of ϕ for each set of χ are obtained by the requirement that the chemical potentials are the same in each phase.

To evaluate the partition function and, hence, determine the free energy, we use the numerical mean-field method of Hong and Noolandi.[11] This method is now standard so we summarize the steps here and leave the details to the appendix. The partition function is evaluated via a saddle functional method with the constraint of local incompressibility, $\sum_p \phi_p(\mathbf{r}) = 1$. A set of extremization conditions is obtained for the local polymer volume fraction $\phi_p(\mathbf{r})$, for a conjugate potential $\omega_p(\mathbf{r})$, and for the Lagrange multiplier function needed to enforce the incompressibility. In general, these equations cannot be solved analytically but must be solved numerically via an iterative method. We also assume that the polymer profile depends only on one direction so that the problem is reduced to solving a set of coupled equations in one dimension.

From this analysis one can obtain the self-consistent polymer profiles $\phi_p(x)$, calculate the free energy of the different solutions and also, if desired, extract more detailed statistical quantities such as the polymer end distribution. For a homogeneous system ($\phi_p(x)$ = constant) the Flory–Huggins free energy is recovered. To study the interfacial behavior, we consider a system of size L and fix the values of ϕ at the edges, $x = 0$ and $x = L$, to be at the two coexistence values. For example, for the A–B interface we would choose the values of ϕ to be given by the A-rich phase coexistence values at $x = 0$ and the B-rich coexistence values at $x = L$. We then solve the extremization equations iteratively with these boundary conditions. To obtain the surface tension, we simply calculate the free energy per unit area of the system with the interface and subtract the bulk contribution.

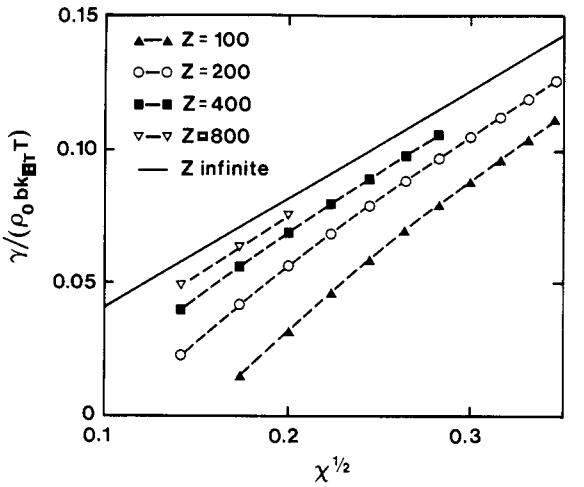

Figure 1. Surface tension for a symmetric two-polymer interface as a function of the Flory parameter χ and polymerization index Z. In the $Z \to \infty$ limit, the surface tension is given by $\gamma = k_B T \rho_0 (\chi/6)^{1/2}$.

III. Two-Component Interface

The first approximation one can make in the treatment of the three-component polymer interface is to ignore the presence of the third component entirely and assume that the surface tensions are the same as that of the pure two-component interfaces. In order to determine the validity of such an approximation, we need the surface tension for the pure two-component interface.

We assume homopolymers of the same degree of polymerization. The interaction energy is given by $W = \rho_0 \int d\mathbf{r}\, \chi\, \phi_A(\mathbf{r})\, \phi_B(\mathbf{r})$ where $\phi_A + \phi_B = 1$. In this case Helfand and Tagami[12] find that in the $Z \to \infty$ limit the surface tension is independent of the chain length and is given by

$$\gamma = k_B T \rho_0 (\chi/6)^{1/2} \quad (3.1)$$

while the interfacial width is proportional to $\chi^{-1/2}$. On the basis of this estimate, the condition for the existence of a macroscopic wetting layer is $\chi_{BC}^{1/2} > \chi_{AB}^{1/2} + \chi_{AC}^{1/2}$ in the infinite chain limit.

However, for the values of Z we consider in the following section, the finite chain effects are very important. We solve for the surface tension for the two-component case using the same numerical method as for the three-component case. Figure 1 shows the surface tension as a function of χ and Z. The infinite chain result of Helfand and Tagami is also plotted. For the three-component case we consider Z from 100 to 200 and the χ's of order 0.05. We will use the values of surface tension from Figure 1 as the reference for the three-component surface tensions.

IV. Three-Component Interfaces

A. General Results. In this section we will consider some general results. Figure 2 shows the polymer profiles obtained for $Z = 100$, $\chi_{AB} = 0.03$, $\chi_{BC} = 0.09$, and $\chi_{AC} \approx 0.062$. These values of χ were chosen because they are on the phase boundary between complete and partial wetting.

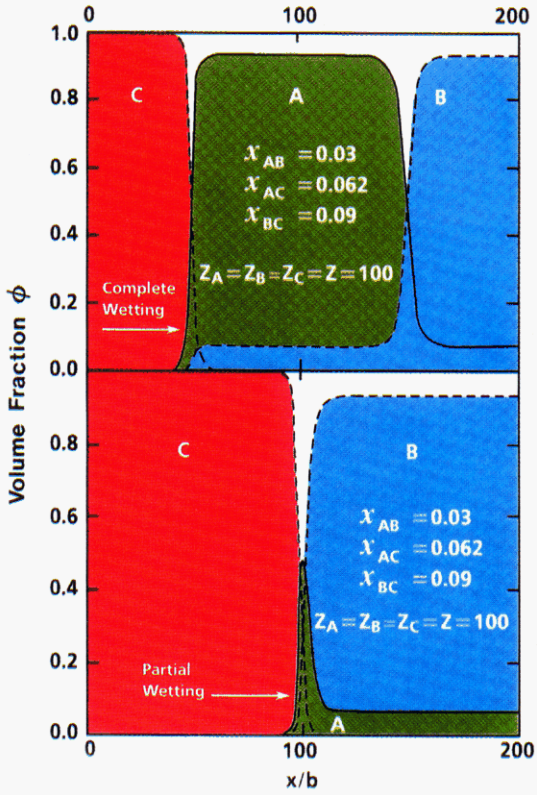

Figure 2. Polymer concentration profiles for $Z = 100$, $\chi_{AB} = 0.03$, $\chi_{BC} = 0.09$, and $\chi_{AC} = 0.062$. These values correspond to the phase boundary between complete and partial wetting. The upper panel shows the complete wetting profile in which there is a macroscopic layer of the A-rich phase between the C- and B-rich phases. The lower panel shows the partial wetting profile. There is a substantial enrichment of A at the B–C interface.

The phase boundary was found by fixing Z, χ_{AB}, and χ_{BC}, slowly decreasing χ_{AC}, and calculating the surface energies of the three interfaces at each value of χ_{AC}. In this way we can follow both the complete wetting and partial wetting profiles. For this set of parameters, we found that $\gamma_{AC} + \gamma_{AB} > \gamma_{BC}$ for $\chi_{AC} > 0.062$ so that the partial wetting solution has a lower free energy. For $\chi_{AC} < 0.062$, $\gamma_{AC} + \gamma_{AB} < \gamma_{BC}$ and the complete wetting profile is the equilibrium phase. For somewhat smaller χ_{AC} the partial wetting branch disappears.

Figure 2 (upper panel) shows the complete wetting profile. This is obtained by joining an A–C interface to an A–B interface. The important thing to note is that, due to large repulsive interaction between B and C, there is almost no C at the A–B interface and only a small overlap of B and C at the A–C interface. The two-component estimate for the surface tension of these two interfaces should be relatively accurate. This is confirmed in Figure 3 where we have plotted, as a function of χ_{AC}, the normalized surface tension of the A–B and A–C interfaces. That is, we divide γ_{AB} and γ_{AC} by the value of the surface tension (γ_2) expected for the pure two-component interface with the same χ value.

The features of the normalized surface tension curve for the A–C interface are interesting. As χ_{AC} is increased toward χ_{BC}, the interaction energy cost of B–C overlap relative to A–C overlap is decreased. The presence of the third component at the interface increases the entropy, thereby providing a small reduction ($\approx 2\%$) in the interfacial energy. For smaller values of χ_{AC} the small but nonzero B–C overlap actually increases the surface tension slightly above the two-component estimate. However, these effects are very small and the surface tension of the

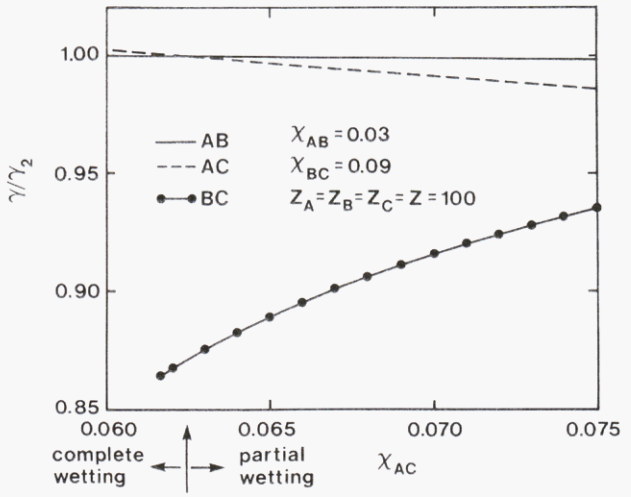

Figure 3. Surface energy per unit area of the three-component interfaces γ divided by γ_2, the value expected for the pure two-component interface, plotted as a function of χ_{AC} for $Z = 100$, $\chi_{AB} = 0.03$, and $\chi_{BC} = 0.09$. The arrow marks the phase boundary between the complete wetting phase (smaller χ_{AC}) and the partial wetting phase (larger χ_{AC}).

A–C interface is essentially that of the pure two-component interface.

Figure 2 (lower panel) shows the partial wetting profile, i.e., the B–C interface. Since χ_{BC} is larger than χ_{AC} and χ_{AB}, the surface energy can be reduced by increasing the amount of A–C and A–B contact and thereby reducing the B–C contact. Therefore, there is an enrichment of the A phase at the B–C interface. This is in contrast to the complete wetting interfaces where there is no enrichment of the third phase (C at the A–B interface and B at the A–C interface) at the two interfaces. For example, ϕ_A^{max}, the maximum value of ϕ_A at the interface for partial wetting is 0.48 while the value of ϕ_A in the B-rich phase is 0.07. This effect leads to a substantial reduction in the surface tension of the B–C interface (relative to the two-component prediction) as χ_{AC} is reduced. As shown in Figure 3, the surface tension is reduced by 13% at the wetting transition. For smaller values of χ_{BC} (at the same values of χ_{AB} and Z) the fractional reduction of the surface tension at the wetting transition can be much larger. For $\chi_{BC} = 0.07$, the fractional reduction is 21% at the wetting transition.

The net effect is that the values of χ_{AC} for which the partial wetting branch is stable is increased relative to the two-component estimate. For this set of values, the two-component estimate would predict that the complete wetting branch would be stable for $\chi_{AC} < 0.073$, while the full three-component solution predicts that the partial wetting branch is stable down to $\chi_{AC} > \chi^*_{AC} = 0.062$.

Although we have discussed the result for a specific set of parameters, the arguments given in this subsection are general. For general values of χ_{AB}, $\chi_{AC} < \chi_{BC}$, we find that the third component is repelled from the A–C and A–B interfaces due to the larger value of χ_{BC}. Therefore, the surface energy for the macroscopic wetting profile is essentially given by the two-component estimates. On the other hand, there is a large enrichment of the A phase at the B–C interface. This reduces the surface tension relative to the pure two-component estimate and increases the regime of χ_{AC} in which the partial wetting branch has the lower surface energy.

B. The Wetting Transition. To further investigate the wetting transition, we repeat the process described in

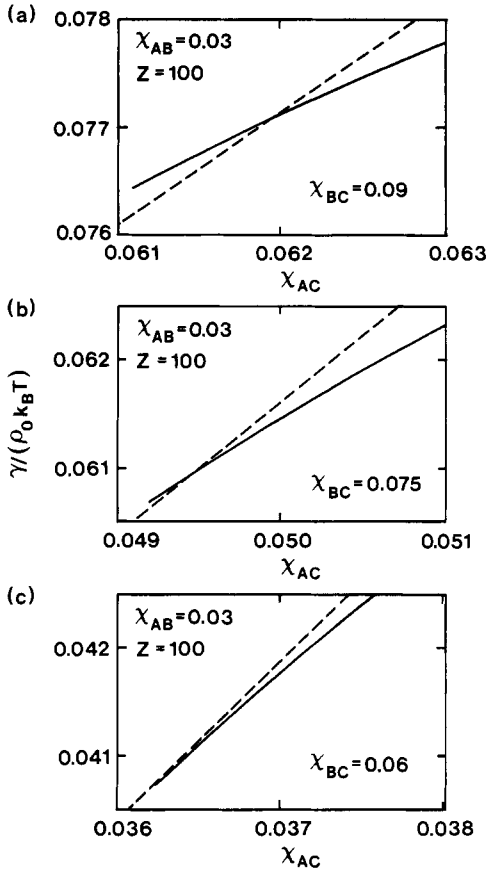

Figure 4. Surface energy per unit area for the complete wetting branch (dashed line) and the partial wetting branch (solid line) as a function of χ_{AC} for $Z = 100$, $\chi_{AB} = 0.03$, and (a) $\chi_{BC} = 0.09$, (b) $\chi_{BC} = 0.075$, and (c) $\chi_{BC} = 0.06$. The two branches for the surface energies cross for $\chi_{BC} = 0.09$ and $\chi_{BC} = 0.075$ but seem to approach each other tangentially for $\chi_{BC} = 0.06$.

the previous subsection for different values of χ_{BC}. That is, we fix $\chi_{AB} = 0.03$ and $Z = 100$. This effectively fixes the value of ϕ_A in the host B-rich matrix. Then for different values of χ_{BC} we slowly increase the value of χ_{AC} following both the complete wetting and partial wetting branches. We calculate the polymer profiles and surface energies at each value of χ_{AC}. In this way we determine the value of χ_{AC} at which the stability of the two branches is interchanged for each set of χ_{AB}, χ_{BC}, and Z.

Figure 4 shows the surface energy per unit area of the partial and complete wetting solutions as a function of χ_{AC} for $\chi_{BC} = 0.06$, 0.075, and 0.09. Note that for $\chi_{BC} = 0.075$ and $\chi_{BC} = 0.09$ there is a clear crossing of the two surface energies as a function of χ_{AC} but the angle at which the curves cross is smaller for smaller χ_{BC}. For $\chi_{BC} = 0.06$ (Figure 4c) the two branches seem to approach each other tangentially. However, it is difficult to pinpoint the exact value of χ_{AC} at which the surface energies of the two branches are equal since the numerical convergence becomes increasingly difficult as that value is approached. Therefore, we cannot be certain for $\chi_{BC} = 0.06$ whether the approach of the two curves is exactly tangential or if they actually cross one another.

Figure 5 shows ϕ_A^{max}, the maximum value of ϕ_A, for the two branches as a function of χ_{AC} for the same set of χ_{BC}'s as in Figure 4. For the two larger values of χ_{BC} it is clear that there is a discontinuous jump in ϕ_A^{max} as the stability of the branches is interchanged. Figures 4 and 5 therefore show that the phase transition is first order for these values of χ_{BC}. For $\chi_{BC} = 0.06$ the result is less clear-cut. Since we do not know the exact value of χ_{AC} at the wetting

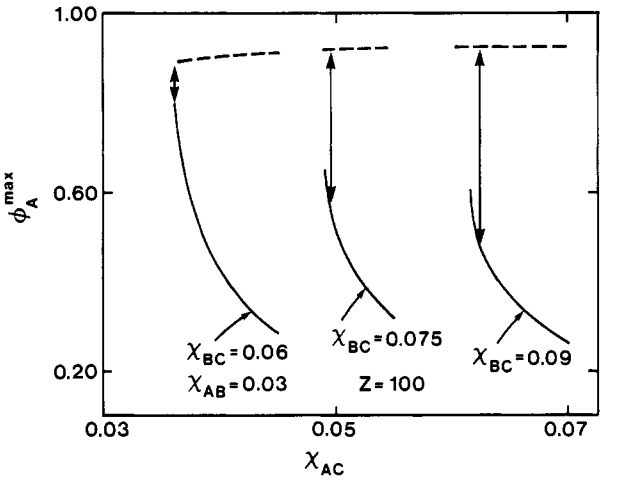

Figure 5. Value of ϕ_A^{max} for the complete wetting (dashed line) and partial wetting (solid line) profiles as a function of χ_{AC} for $\chi_{BC} = 0.06$, 0.075, and 0.09. The arrows indicate the phase transition points. For $\chi_{BC} = 0.06$ the line indicates where the surface energies of the two branches are within 0.1% of one another.

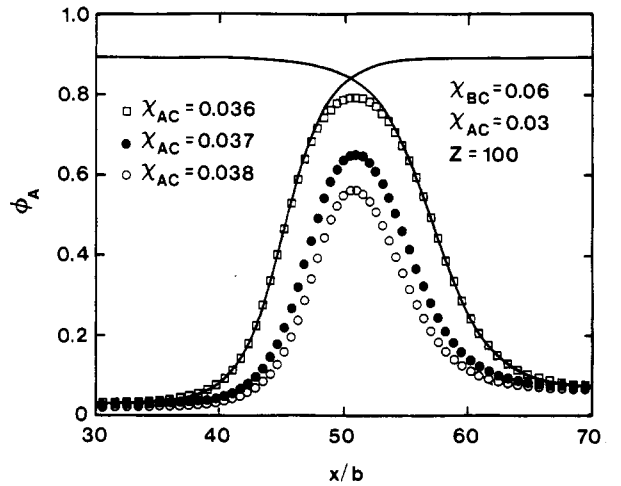

Figure 6. $\phi_A(x)$ for the partial wetting solution near the possible second-order phase transition point for $\chi_{BC} = 0.06$, $\chi_{AC} = 0.03$, and $Z = 100$. The profiles for $\chi_{AC} = 0.036$, 0.037, and 0.038 are shown. The solid lines show $\phi_A(x)$ for the A–B and A–C interfaces. These have been translated so they fall onto the B–C interface. It is seen that $\phi_A(x)$ converges to the complete wetting result as χ_{AC} is decreased.

transition, we cannot tell whether there is a discontinuous jump in ϕ_A^{max}. However, the fact that ϕ_A^{max} increases rapidly with decreasing χ_{AC} before the phase transition indicates that the jump is very small. This is shown in Figure 6 where we plot $\phi_A(x)$ for the B–C interface for several values of χ_{AC} near the transition. We also show $\phi_A(x)$ for the A–B and A–C interfaces. These two interfaces have been translated so that they fall on top of the B–C interface. It is seen that the polymer profile for the B–C interface is approaching that of the combination of the A–B and A–C interface. Thus, it is not surprising that this profile has a surface energy very close to that of the macroscopic wetting profile and therefore that the surface energies of the wetting and partial wetting profiles approach each other tangentially. Although, within the numerical mean-field method, we cannot state conclusively that there exists a continuous transition, these results along with the evidence to be discussed below indicate that the wetting transition is continuous for $\chi_{BC} = 0.06$. We find that the results for $\chi_{BC} = 0.055$ and $\chi_{BC} = 0.065$ are also consistent with a second-order phase transition.

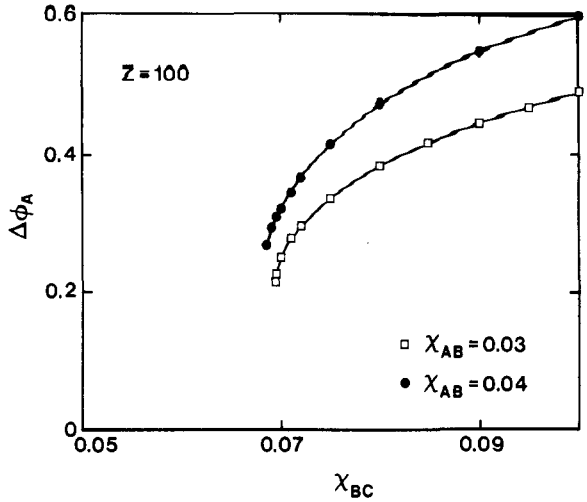

Figure 7. Discontinuity in ϕ_A^{max} at the wetting transition as a function of χ_{BC}. Results for $\chi_{AB} = 0.03$ and $\chi_{AB} = 0.04$ are shown. Note that for $\chi_{AB} = 0.03$ there is a rapid decrease in $\Delta\phi_A$ near $\phi_{BC} = 0.07$. For $\chi_{AB} = 0.04$ the rapid decrease occurs at a slightly smaller value of χ_{BC}.

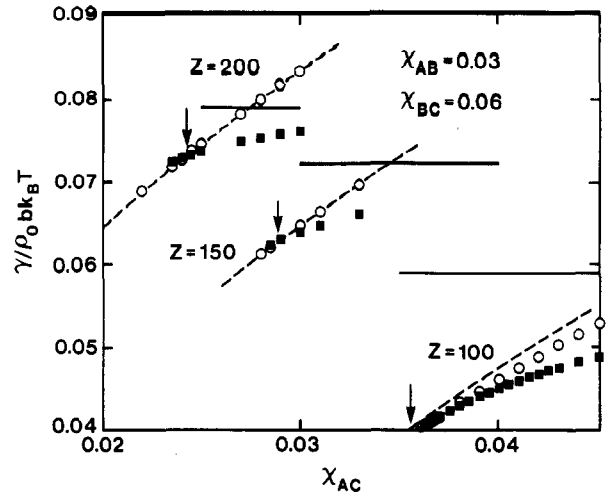

Figure 8. Surface energy per unit area for the complete wetting branch (solid squares) and the partial wetting branch (open circles) as a function of χ_{AC} for $\chi_{AB} = 0.03$ and $\chi_{BC} = 0.06$ for $Z = 100$, 150, and 200. The arrow indicates the wetting transition for each Z. For each Z, the dashed line corresponds to the two-component estimate for the complete wetting branch and the solid line to the two-component estimate for the partial wetting branch.

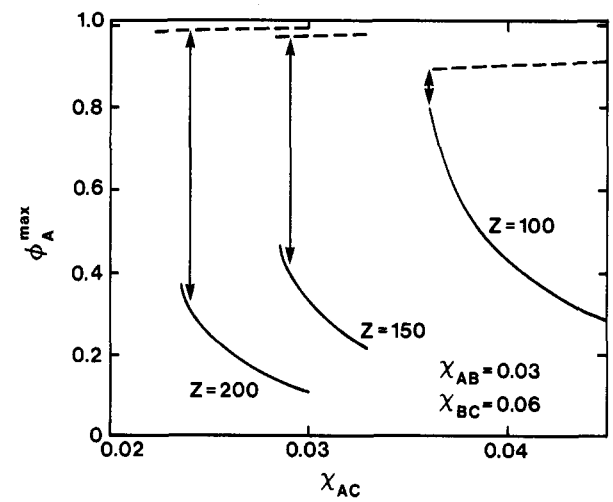

Figure 9. Value of ϕ_A^{max} for the complete wetting (dashed line) and partial wetting (solid line) profiles as a function of χ_{AC} for $Z = 100$, 150, and 200 and $\chi_{AB} = 0.03$ and $\chi_{BC} = 0.06$. The arrows indicate the phase transition points. For $Z = 100$ the line indicates where the surface energy of the two branches are within 0.1% of one another.

Figure 7 shows $\Delta\phi_A^{max}$, the jump in ϕ_A^{max} at the transition as a function of χ_{BC}. Results for $\chi_{AB} = 0.03$ and $\chi_{AB} = 0.04$ are shown. From the figure we see that there is a rapid drop in $\Delta\phi_A^{max}$ at approximately $\chi_{BC} = 0.695$ for $\chi_{AB} = 0.03$ and $\chi_{BC} = 0.068$ for $\chi_{AB} = 0.04$. This result combined with the previous analysis indicates that these are the dividing lines between the first- and second-order phase transitions. For example, for $\chi_{AB} = 0.03$, the wetting transition is first order for $\chi_{BC} \gtrsim 0.069$ and second order for $\chi_{BC} \lesssim 0.069$. A similar result holds for $\chi_{AB} = 0.04$, with the dividing line between the first- and second-order wetting transitions being at approximately $\chi_{BC} \approx 0.068$. For interactions with rigid walls, second-order phase transitions are relatively rare and the wall interactions are difficult to characterize.[10] Critical wetting for a binary fluid with long-range interactions in three-phase coexistence with its vapor has been predicted by Dietrich and Schick.[13] Our result indicates that a large regime of second-order wetting transition may be obtained for these three-component blends, possibly providing useful systems to investigate second-order wetting transitions.

C. Z Dependence. To study the behavior as a function of the polymerization index Z, we fix $\chi_{AB} = 0.03$ and $\chi_{BC} = 0.06$ to determine the polymer profiles and behavior of the wetting transition for $Z = 100$, 150, and 200. Figure 8 shows a plot of the surface energy of the complete wetting and partial wetting branches of the free energy vs χ_{AC} for different values of Z. Also shown on this plot are the estimates of the surface energy based on the pure two-component interfaces. The point where the branches cross corresponds to the wetting transition.

Several important features are to be noted. First, as Z increases, the wetting transition is pushed toward smaller values of χ_{AC}. This is simply because γ_{AB} increases by a larger proportional amount than the surface tensions of the other interfaces. In fact, in the infinite Z limit, the two-component estimate would predict that the transition occurs at $\chi_{AC} = 0.005$. Second, we find that as Z is increased the surface energy estimate for the complete wetting branch becomes extremely accurate. For $Z = 150$ one sees hardly any difference between the two-component estimate and the three-component result on this plot. Third, the wetting transition is always at a slightly smaller value of χ_{AC} than predicted by the two-component estimate because, as discussed earlier, there is a reduction of γ_{BC} from its two-component value which increases the regime of partial wetting. However, we find that the fractional reduction is also becoming smaller as Z is increased. The result is that with increasing Z the two-component estimate for the transition becomes more and more accurate (at least at fixed χ_{AB} and fixed χ_{BC}).

As Z is increased, the angle at which the two branches of the surface energy cross also increases. The transition becomes more strongly first order with increasing Z. This is confirmed in Figure 9 in which we show a plot of ϕ_A^{max} for the two branches as a function of χ_{AC} for different values of Z. For $Z = 100$ the transition is seemingly second order. However, the jump becomes larger with increasing Z. This result can be understood as follows. For fixed χ_{AB}, the volume fraction ϕ_A in the host B-rich phase is a decreasing function of Z and there is less of the A phase to pull in from the background. This reduces the effective enrichment of A at the interface and makes the discon-

tinuity at the transition larger as well as the transition more strongly first order with increasing Z.

We conclude that, for fixed χ_{AB}, the two-component estimate will become increasingly accurate with increasing Z. Note that this would not be true if we increased Z with $\chi_{AB}Z$ fixed, i.e., holding the background concentration of ϕ_A fixed. In this case we would expect a large enrichment of A at the interface and a corresponding reduction in the B–C surface tension.

V. Summary

We have investigated the wetting behavior of a three-component (A–B–C) polymer blend using a numerical self-consistent mean-field method. We find that a wetting transition can occur in which one of the minority phases (A) wets the other. First, we determine how the presence of the third component affects the behavior of the interface between two phases. We calculate the polymer profiles and find a substantial enrichment of the A phase at the B–C interface. This leads to a significant reduction of the interfacial tension and extends the partial wetting regime relative to what is expected from a simple two-component estimate. Second, we find the existence of first-order wetting transitions and our results indicate that a second-order wetting transition may also be possible. We discuss how the phase boundary varies as a function of the microscopic parameters. Finally, we discuss the polymerization dependence. We find that as Z is increased the transition becomes increasingly first order and the two-component estimate become more precise. However, we note that the infinite Z limit is somewhat subtle. If Z is increased with χ_{AB} fixed, the wetting transition becomes increasingly first order due to the reduction of the minority phase in the bulk. However, if Z is increased with the product $\chi_{AB}Z$ fixed, the opposite would occur. There will continue to be a substantial reduction in the B–C surface tension. This will result in an increase in the regime in which the wetting transition seems to be second order.

Here we conjecture on the difference between polymeric and simple liquids in regards to the wetting behavior. The existence of the second-order wetting transition depends crucially on the reduction of the surface tension of the partial wetting interface due to the presence of the third polymer. As was shown here and in ref 2 polymeric systems produce a significantly larger decrease in surface tension than for simple liquids. This is mainly because of the smaller role that the configurational entropy plays for large macromolecules than for small molecules. This does not contradict our result that the transition becomes increasing first order with increasing Z, since here we assume increasing Z with fixed bulk volume fraction of the minority phase.

The ideas used here should be applicable even to systems which are not in global equilibrium. This is because the times required to achieve global equilibrium may be so long that it is never reached in practice. However, the interfaces between polymers should approach local equilibrium fairly quickly. Then the approach presented in this paper should give a good description for the experiment of Hobbs et al.[6] for melt blends of homopolymers, provided that the χ parameters can be determined accurately.

Acknowledgment. We thank Dr. A. C. Shi for useful discussions. This work was partially supported by Natural Sciences and Engineering Research Council.

Appendix A: The Numerical Mean-Field Method

1. **Mean-Field Approximation.** The partition function for a multicomponent polymer blend is given by

$$Z = \prod_p \left\{ \frac{Z_{p,\mathrm{kin}}^{N_p}}{N_p!} \right\} \int \{ \prod_p \prod_{j=1}^{N_p} \mathcal{D}\{\mathbf{R}_{pj}\} P_0[\mathbf{R}_{pj}] \exp(-W) \}$$

Here the index p is A, B, or C and denotes the type of polymer. The contour of the jth polymer of type p is given by $\{\mathbf{R}_{pj}\}$ and $Z_{p,\mathrm{kin}}$ is the factor due to kinetic energy for a chain of type p. The probability functional for a given space curve is given by $P_0[\mathbf{R}_{pj}(\bullet)]$ and is assumed to be the standard Weiner form, i.e.

$$P_0[\mathbf{R}_{pj}(\bullet)] \propto \exp\left[-\frac{3}{2b^2} \int_0^{Z_p} dt \left(\frac{\partial \mathbf{R}_{pj}}{\partial t} \right)^2 \right] \quad \text{(A1)}$$

Here the Kuhn length b is the same for all species and Z_p is the polymerization of a chain of type p. The interaction energy (in units of k_BT) is $W = \rho_0 \int d\mathbf{r}\, f(\phi(\mathbf{r}))$ where the interaction energy per monomer f is given by eq 2.1, $f(\phi) = \chi_{AB}\phi_A\phi_B + \chi_{AC}\phi_A\phi_C + \chi_{BC}\phi_B\phi_C$. Here ρ_0 is the density of the pure polymer in units of monomer segments per unit volume and χ's are the Flory interaction parameters.

The local volume fraction can be written as a functional of the chain contours

$$\rho_0 \phi_p(\mathbf{r}) = \sum_{j=1}^{N_p} \int dt\, \delta(\mathbf{r} - \mathbf{R}_{pj}(t))$$

Using the integral representation of $\delta(\mathbf{r})$, Z can be written as a functional of $\phi_p(\mathbf{r})$,

$$Z = \int \mathcal{D}\{\phi_p(\bullet)\} \int \mathcal{D}\{\omega_p\} \exp(-F[\{\phi_p(\bullet)\},\{\omega_p(\bullet)\}]) \quad \text{(A2)}$$

where

$$F[\{\phi_p\},\{\omega_p\}] = W\{\phi\} - \sum_p \rho_0 \int d\mathbf{r}\, \omega_p(\mathbf{r})\, \phi_p(\mathbf{r}) + \sum_p \rho_0 \int d\mathbf{r}\, \frac{\phi_p(\mathbf{r})}{Z_p} \left(\ln\left[\frac{N_p}{\rho_0 Z_{\mathrm{kin},p} Q_p} \right] - 1 \right) \quad \text{(A3)}$$

Q_p is the partition function for a single non-self-avoiding chain of species p in potential $\omega_p(\mathbf{r})$,

$$Q_p = \int \mathcal{D}\{\mathbf{R}_{pj}\} \exp\left(-\int_0^{Z_p} dt \left[\frac{3}{2b^2} \left(\frac{\partial \mathbf{R}_{pj}(t)}{\partial t} \right)^2 + \omega_p(\mathbf{R}_{pj}(t)) \right] \right)$$

$$= \int d\mathbf{r} \int d\mathbf{r}_0\, Q_p(\mathbf{r},Z_p|\mathbf{r}_0) = \int d\mathbf{r}\, q_p(\mathbf{r},Z_p) \quad \text{(A4)}$$

The Green function $Q_p(\mathbf{r},t|\mathbf{r}_0)$ is the primary quantity of interest and obeys the diffusion equation

$$\frac{\partial Q_p(\mathbf{r},t|\mathbf{r}_0)}{\partial t} = \frac{b^2}{6} \nabla^2 Q_p(\mathbf{r},t|\mathbf{r}_0) - \omega_p(\mathbf{r})\, Q_p(\mathbf{r},t|\mathbf{r}_0) \quad \text{(A5)}$$

We define $\bar{\phi}_p \equiv V^{-1} \int d\mathbf{r}\, \phi_p(\mathbf{r})$ and $\bar{\omega}_p$ via

$$Q_p = V \exp(-Z_p \bar{\omega}_p) \quad \text{(A6)}$$

where V is the volume of the system. We rewrite $F[\{\phi_p(\bullet)\},\{\omega_p(\bullet)\}]$ as

$$F[\{\phi_p(\bullet)\},\{\omega_p(\bullet)\}] = W\{\phi\} - \sum_p \rho_0 \int d\mathbf{r}\, \delta\omega_p(\mathbf{r})\, \phi_p(\mathbf{r}) + \sum_p N_p \left(\ln\left[\frac{N_p}{\rho_0 V Z_{\mathrm{kin},p}} \right] - 1 \right) \quad \text{(A7)}$$

where $\delta\omega_p(\mathbf{r}) \equiv \omega_p(\mathbf{r}) - \bar{\omega}_p$.

To this point there are no approximations other than those used to obtain the initial model. To proceed further, we make the mean-field approximation by performing the functional integrations in eq A2 using the saddle function method. This must be done with the constraint of local incompressibility of the polymer mixture.

$$\sum_p \phi_p(\mathbf{r}) = 1 \tag{A8}$$

Note that, since the partition function is already written with N_p fixed, we do not need an additional Lagrange multiplier for this constraint. In fact, if we include this constraint, we simply obtain a set of arbitrary constants λ_p which can be absorbed into ω_p.

To carry out the extremization of the free energy with this constraint, we introduce the Lagrange multiplier function $\eta(\mathbf{r})$. The function to extremize becomes

$$F[\{\phi_p(\bullet)\},\{\omega_p(\bullet)\}] + \int d\mathbf{r}\, \eta(\mathbf{r})\,(\sum_p \phi_p(\mathbf{r}) - 1) \tag{A9}$$

Extremizing with respect to $\omega_p(\mathbf{r})$, we obtain

$$\rho_0\phi_p(\mathbf{r}) = -\frac{N_p}{Q_p\{\omega_p\}}\frac{\delta Q_p}{\delta\omega_p(\mathbf{r})}$$

$$= \frac{N_p}{Q_p}\int_0^{Z_p} dt\; q_p(\mathbf{r},t)\; q_p(\mathbf{r},Z_p-t) \tag{A10}$$

Extremizing with respect to $\phi_p(\mathbf{r})$ gives

$$\rho_0\omega_p(\mathbf{r}) = \frac{\partial W}{\partial\phi_p(\mathbf{r})} + \eta(\mathbf{r}) \tag{A11}$$

There is one arbitrary constant which we set by fixing $\eta(\mathbf{r}) = 0$ at one of the boundaries. Note that expression (A10) is independent of $\bar{\omega}_p$ but depends only on $\delta\omega_p(\mathbf{r})$.

In the mean-field approximation the free energy becomes

$$F[\{\phi_p(\bullet)\},\{\omega_p(\bullet)\}] = W\{\phi\} - \sum_p \rho_0\int d\mathbf{r}\, \delta w_p(\mathbf{r})\, \phi_p(\mathbf{r}) +$$

$$\sum_p \rho_0\int d\mathbf{r}\,\frac{\phi_p(\mathbf{r})}{Z_p}\ln\bar{\phi}_p - \sum_p N_p(\ln(Z_pZ_{\mathrm{kin},p}) + 1) \tag{A12}$$

where $\phi_p(\mathbf{r})$ and $\omega_p(\mathbf{r})$ are the solutions to the extremum equations and we have used $N_p = \rho_0\int d\mathbf{r}\, \phi_p(\mathbf{r})/Z_p$. Note that the last term can be absorbed into chemical potentials in $W\{\phi\}$.

For a homogeneous system $\delta\omega_p = 0$ and $\phi_p(\mathbf{r}) = \bar{\phi}_p$ and the standard Flory–Huggins free energy is recovered. For example, for a two-component symmetric polymer system, the free energy per monomer is

$$\frac{F}{\rho_0 V} = \chi\phi_A\phi_B + \frac{\phi_A}{Z}\ln\phi_A + \frac{\phi_B}{Z}\ln\phi_B \tag{A13}$$

where $\phi_A + \phi_B = 1$ and we have neglected constant terms.

2. Surface Tension. To calculate the surface tension, we consider a system of size L in the x direction. First, the values of ϕ at coexistence are obtained from the bulk three-component Flory–Huggins free energy with the requirement that chemical potentials are the same in each phase. (As noted in the previous subsection this method recovers the bulk Flory–Huggins free energy for the homogeneous system.) We fix the interface to be at $x = L/2$ and assume that the polymer concentration is homogeneous in the y–z directions. The values of ϕ at the edges, $x = 0$ and $x = L$, are chosen to be at different coexistence values. For example, for the AB interface we would choose the values of ϕ to be given by A-rich phase coexistence value at $x = 0$ and the B-rich phase at $x = L$.

The surface tension is then given by

$$\gamma = \rho_0\int dx\, [f(\phi(x)) + \mu_A\phi_A(x) + \mu_B\phi_B(x)] -$$

$$\rho_0\int dx\, [\delta\omega_A(x)\,\phi_A(x) + \delta\omega_B(x)\,\phi_B(x) + \delta\omega_C(x)\,\phi_C(x)] +$$

$$\rho_0\int dx\left[\frac{\phi_A(x)}{Z}\ln\bar{\phi}_A + \frac{\phi_B(x)}{Z}\ln\bar{\phi}_B + \frac{\phi_C(x)}{Z}\ln\bar{\phi}_C\right] - \rho_0\int dx\, f_{\mathrm{bulk}} \tag{A14}$$

where the chemical potentials μ_A and μ_B are needed to remove the bulk contributions. The bulk free energy per monomer f_{bulk} is given by

$$f_{\mathrm{bulk}} = f(\phi(x)) + \mu_A\phi_A(x) + \mu_B\phi_B(x) - \delta\omega_A(x)\,\phi_A(x) -$$

$$\delta\omega_B(x)\,\phi_B(x) - \delta\omega_C(x)\,\phi_C(x) + \frac{\phi_A(x)}{Z}\ln\phi_A(x) +$$

$$\frac{\phi_B(x)}{Z}\ln\phi_B(x) + \frac{\phi_C(x)}{Z}\ln\phi_C(x) \tag{A15}$$

where x can be either 0 or L.

3. Computational Algorithm. We implement the mean-field method for the three-component polymer blend as follows:

1. For each set of values of Z and χ_{AB}, χ_{AC}, and χ_{BC}, we determine the values of ϕ and μ corresponding to the three coexisting states.

2. Make an initial guess for ω_A, ω_B, and ω_C.

The values of ω_p at the boundaries are set by fixing $\eta(0) = 0$ so that, from eq A10, 23 have $\rho_0\omega_p(0) = \partial W/\partial\phi_p(0)$ at $x = 0$. We assume that the other boundary is far into the bulk. Then the value $x = L$ is given by

$$\omega_p(L) = \omega_p(0) + \frac{1}{Z}\ln\left(\frac{\phi_p(0)}{\phi_p(L)}\right)$$

For the initial condition, either we can use values of ω_p which converge for parameters χ close to the present values and rescale ω_p so that the above boundary conditions are met or we start with an entirely new initial condition. To make a new initial condition, we set $\omega_p(x) = \omega_p(0)$ for $x < L/2$ and $\omega_p(x) = \omega_p(L)$ for $x > L/2$. We set $\omega_p(L/2) = (\omega_p(0) + \omega_p(L))/2$.

For the partial wetting solution (C–B interface) we choose $\phi_p(0)$ to be in the C-rich phase and $\phi_p(L)$ to be in the B-rich phase. We make the complete wetting solution in two steps. First, we choose $\phi_p(0)$ to be in the C-rich phase and $\phi_p(L)$ to be in the A-rich phase to obtain the A–C interface profile. We next choose $\phi_p(0)$ to be in the A-rich phase and $\phi_p(L)$ to be in the B-rich phase to obtain the A–B interface. We then combine the two interfaces to obtain the complete wetting solution. A check is made that the combined interfaces are a solution to the mean-field extremum equations.

3. Solve eq A11 using $\omega_p(x)$ to obtain $\rho_p(x)$. In general the incompressibility condition will not be met. We define

$$\phi'_p(x) \equiv \frac{\phi_p(x)}{\sum_p \phi_p(x)} \tag{A16}$$

so that $\phi'_p(x)$ meets the incompressibility condition.

4. Use eq A10 and $\phi'_p(x)$ to obtain $\eta(x)$ via

$$\eta(x) = \frac{1}{\sum_p \mathrm{wght}_p(x)} \sum_{q=1,3} \mathrm{wght}_q(x) \left(-\left.\frac{\partial W}{\partial \phi_p(x)}\right|_{\phi'} + \rho_0 \omega_p(x) \right) \tag{A17}$$

Here the weight function $\mathrm{wght}_p(x)$ is chosen to be $\mathrm{wght}_p = \min(\phi'_p, 1-\phi'_p)$. This weight function is chosen so that the two-component algorithm would be recovered when the volume fraction of one species of polymers is much less than the other two.

5. Use the value of $\eta(x)$ and the constraint equation (A10) to obtain $\omega'_p(x)$.

$$\rho_0 \omega'_p(x) = -\frac{\partial W}{\partial \phi_p(x)} + \eta(x) \tag{A18}$$

This would be used to obtain the new guess. However, it is found that we can enhance the convergence by adding an extra term to push the potentials toward incompressibility. We define

$$\omega''_p(x) \equiv \omega'_p(x) - \alpha(1 - \sum_q \phi_q(x))$$

where $1 \geq \alpha \geq 0$. It is clear that, if $\sum_q \phi_q > (<) 1$, then $\omega''_p > (<) \omega'_p$ and the concentration is reduced (increased) on the next iteration. The original constraint equation is recovered when the local incompressibility constraint is met.

6. Use $\omega''_p(x)$ to make the next guess for $\omega_p(x)$ using either

$$\omega_p(x) \rightarrow \omega_p(x) + \delta(\omega''_p(x) - \omega_p(x)) \tag{A19}$$

or the modified secant method. In practice it is found that convergence is enhanced by switching from one method to the other in the iteration process.

7. Return to step 3 with the new guesses for ω_p and continue until convergence is reached and incompressibility is met. In practice we required that $\int dx\, |\sum_p \phi_p(x) - 1| < 10^{-5}$ and $\int dx\, |\omega_p(x) - \omega'_p(x)| < 10^{-5}$.

The numerical details are given below. We used a system size of $L_x = 100$ (in units of b). We used a nonlinear mesh of 100 points with a finer spacing in the middle near the interface. For the integration over the chain contour in eq A10 we break the chain into 50 points. The Green function equation (eq A5) was integrated using the Crank–Nicholson method with $dt = Z/200$. In general, it was found that the A–B interface converges very quickly. The A–C interface takes somewhat longer and the B–C interface takes an extremely large number of iterations in order to converge when the maximum value of ϕ_A is close to that of the value of ϕ_A in the A-rich phase.

References and Notes

(1) See, for example: Russell, T. P. *Mater. Sci. Rep.* **1990**, *5*, 171.
(2) Helfand, E. *Macromolecules* **1992**, *25*, 1676–1685.
(3) Schmidt, I.; Binder, K. *J. Phys. (Paris)* **1985**, *46*, 1631.
(4) Carmesin, I.; Noolandi, J. *Macromolecules* **1989**, *22*, 1689.
(5) Rowlinson, J. S.; Widom, B. *Molecular Theory of Capillarity*; Oxford University Press: New York, 1989.
(6) Hobbs, S. Y.; Dekkers, M. E. J.; Watkins, V. H. *Polymer* **1988**, *27*, 1598.
(7) Moldover, M. R.; Cahn, J. W. *Science* **1980**, *207*, 1073. Moldover, M. R.; Schmidt, J. W. *Physica* **1984**, *12D*, 351.
(8) Dietrich, S. In *Phase Transitions and Critical Phenomena*; Domb, C., Lebowitz, J. L., Eds.; Academic Press: London, 1988; Vol. 12.
(9) Wortis, M. In *Fundamental Problems in Statistical Mechanics VI*; Cohen, E. G. D., Ed.; North-Holland: Amsterdam, The Netherlands, 1985.
(10) de Gennes, P.-G. *Rev. Mod. Phys.* **1985**, *57*, 827.
(11) Hong, K. M.; Noolandi, J. *Macromolecules* **1981**, *14*, 747.
(12) Helfand, E.; Tagami, Y. *J. Chem. Phys.* **1972**, *56*, 3592.
(13) Dietrich, S.; Schick, M. *Phys. Rev. B* **1986**, *33*, 4952; **1989**, *40*, 9204.